

# GNNBleed: Inference Attacks to Unveil Private Edges in Graphs with Realistic Access to GNN Models

Zeyu Song  
Penn State University

Ehsanul Kabir  
Penn State University

Shagufta Mehnaz  
Penn State University

## Abstract

Graph Neural Networks (GNNs) have increasingly become an indispensable tool in learning from graph-structured data, catering to various applications including social network analysis, recommendation systems, etc. At the heart of these networks are the edges which are crucial in guiding GNN models' predictions. In many scenarios, these edges represent sensitive information, such as personal associations or financial dealings— thus requiring privacy assurance. However, their contributions to GNN model predictions may in turn be exploited by the adversary to compromise their privacy. Motivated by these conflicting requirements, this paper investigates edge privacy in contexts where adversaries possess black-box GNN model access, restricted further by access controls, preventing direct insights into arbitrary node outputs. In this context, we introduce a series of privacy attacks grounded on the message-passing mechanism of GNNs. These strategies allow adversaries to deduce connections between two nodes not by directly analyzing the model's output for these pairs but by analyzing the output for nodes linked to them. Our evaluation with seven real-life datasets and four GNN architectures underlines a significant vulnerability: even in systems fortified with access control mechanisms, an adaptive adversary can decipher private connections between nodes, thereby revealing potentially sensitive relationships and compromising the confidentiality of the graph.

## 1 Introduction

Graph Neural Networks (GNNs) are a class of deep learning models designed to handle graph-structured data [4, 34, 44, 46]. Unlike traditional neural networks that assume data is structured in a grid-like manner (e.g., images) or in sequences (e.g., time series or text), GNNs are designed for data where entities (nodes) and their relationships (edges) are explicitly represented as a graph. With applications as diverse as pioneering protein folding methods in AlphaFold [17], reimagining recommendation algorithms for social networks [11, 40, 43], and

detecting security threats in computer systems [23, 34, 37], GNNs continue to shape multiple technological frontiers.

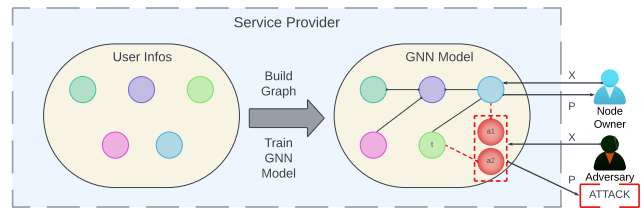


Figure 1: Users/clients interaction with the GNN model.

Edge in a graph often denote sensitive information, such as friendship in a social network or transaction in a financial analysis network [11, 26]. Unveiling these connections without consent infringes upon the privacy of the entities involved. Understanding edge inference attacks is crucial to comprehending the vulnerabilities inherent within GNNs, and thereby, devising mechanisms to preserve privacy by safeguarding these relationships.

Previous research [13, 42] has exposed edge privacy vulnerabilities in GNN models. These investigations, however, hinge on the presumption of the adversary's unconstrained access to the GNN model. For instance, in the link stealing attack (LSA) [13], the adversary can query on any node for model predictions. Concurrently, the LinkTeller attack (LTA) [42] presupposes adversary control over all node features, enabling them to interact with the model using modified features. These techniques predominantly rely on leveraging model predictions for distinct node pairs to infer their connections. Nonetheless, real-world conditions often render such extensive adversary access unrealistic [6], especially considering prevalent access control methods. Addressing this gap, our research explores the possibility of inferring private edges with only practical access to GNN models. We consider a scenario where the service provider uses a private graph to train a GNN model and use it for predictions. Clients represent nodes whereas edges represent their interrelations. Clients can ac-

cess predictions only on their nodes, reflecting practical access restrictions. However, they can alter the graph by changing their features or adding nodes and edges [3,33,38,59,60]. This scenario is analogous to practical environments, for instance, social networks where users update profiles, befriend others, or create new accounts, influencing the graph [1,4,15,49]. The interactions between users and the service provider are shown in Figure 1. **Problem and Scope.** In this paper, we investigate the privacy concerns surrounding a graph’s adjacency information, emphasizing the disclosure of private edges between nodes. We focus on inductive GNNs [12,27,48] as opposed to transductive GNNs due to the former’s ability to generalize to unseen nodes, making them more practical. Our proposed adversarial model endeavors to reveal the neighboring nodes connected to a specific target. Consider a financial network where each node signifies a distinct entity and edges denote transactions between them [6,26]. In such a network, an adversary’s goal might be to uncover the full scope of an entity’s transactions, detailing its financial interactions. Unlike prior work [13,42], in our settings, an adversary operates under constrained circumstances, lacking the privilege to freely query the model regarding all nodes. This restriction amplifies the challenge and drives our exploration into whether sensitive edge information can indeed be compromised, even when direct interaction with the target nodes is off-limits.

**Challenges.** In our context, the primary challenge is the absence of direct access to the model output of targeted node pairs. This limitation necessitates a reliance on indirect information, escalating the complexity of any potential attack. Additionally, the inherent diversity in graph structures adds layers of difficulty. The efficacy of an attack strategy can vary significantly across datasets due to the inconsistencies in graph density and edge interpretations. Moreover, the quest for a generalized attack strategy capable of delivering consistent performance across diverse GNN models persists.

**Key Intuition and New Attacks.** To address the challenges above, we propose a series of attacks that exploit the message aggregation process within GNNs. In GNNs, messages are aggregated among nodes hailing from the same neighborhoods; each node aggregates information from its neighbors to construct its final representation (i.e. posterior). This mechanism paves the way for the possibility of inferring private node attributes even without direct access to the targeted nodes. In GNNs, the exchange of information is inherently bidirectional. A node doesn’t just assimilate information from its neighbors; it also contributes information to them. This dynamic allows for two intuitive strategies to exploit the message aggregation process. One approach is to examine the posterior of a specific node as it encapsulates data from its neighboring nodes. The second approach centers on observing a node’s effect within the network, particularly how it influences the model outputs of other nodes that are integrating its information.

In our attack methodologies, the adversary orchestrates attacks utilizing nodes that are connected to the node pairs tar-

geted. These pivotal nodes are referred to as auxiliary nodes. Based on the methodologies employed, we categorize our attacks into two types: similarity-based and influence-based attacks. The former is primarily focused on dissecting the posterior of the auxiliary nodes to extract meaningful patterns of connected nodes, while the latter is centered around discerning how auxiliary nodes exert influence on its surrounding nodes.

We conduct a comprehensive evaluation of our attacks across four widely-recognized inductive GNN models, namely, Graph Attention Network (GAT) [36], Graph Convolutional Network (GCN) [18], Graph Isomorphism Network (GIN) [47], and GraphSAGE [12]. Our assessment spans seven diverse datasets, including Flickr [52], LastFMAsia [29], and Twitch- $\{DE, EN, FR, PT, RU\}$  [28]. The extensive experimentation underscores that our top-performing attacks exhibit potent effectiveness. Moreover, when pitted against state-of-the-art defenses [42], our evaluations reveal a challenging conundrum - striking a harmonious balance between preserving privacy and retaining utility proves to be a formidable endeavor. Through these evaluations, our work illuminates the significant privacy vulnerabilities inherent within popular GNN architectures, alongside the paramount challenges associated with fortifying them against sophisticated inference attacks.

**Contributions.** In this paper, our primary objective is to explore the potential risks to edge privacy posed by Inductive Graph Neural Networks (GNNs). In summary, we make the following contributions.

- ◆ We introduce a novel threat model and present several query-based edge inference attacks specifically tailored for inductive GNNs. Our findings illustrate that it is indeed feasible to infer the neighbors of a targeted node without requiring direct access to that node.
- ◆ We are the first to showcase consistent effectiveness across a diverse range of inductive GNN architectures. We carried out an extensive set of experiments on four popular inductive GNNs across seven datasets. The results indicate that our approach consistently outperforms two state-of-the-art attack methods, emphasizing the considerable edge privacy concerns present in inductive GNNs.
- ◆ We subject our attacks to a variety of defenses, demonstrating the intrinsic challenge of concurrently achieving both privacy and utility against our attacks.

## 2 Preliminaries

### 2.1 Graph Neural Network (GNN)

Graph Neural Network (GNN) is a class of deep learning models designed to handle data structured as graphs [44]. GNNs can be utilized for various tasks within the graph data domain, primarily aligning with three categories: node-level tasks (e.g. node classification [12, 18, 36, 47]), graph-level tasks (e.g.

graph classification [20, 50]), and edge-level tasks (e.g. link prediction [35, 54]). The core ideology of most GNNs revolves around a neighborhood aggregation strategy [5, 44, 55]. This process allows them to generate representations of nodes that capture not only their own features but also the features of their surrounding context within the graph.

Let  $G = (V, E)$  be a graph where  $V$  represents the set of nodes and  $E$  represents the set of edges. We denote the 1-hop neighbors of a node  $v \in V$  as  $\mathcal{N}(v)$ . When generating representation for  $v$ , after performing  $l$  iterations of message-passing and aggregation, node  $v$ 's representation, denoted as  $h_v^l$ , captures structural information within its  $l$ -hop network neighborhood. GNNs typically consist of multiple graph convolution layers, each of which can be described as:

$$h_v^l = f(h_v^{(l-1)}, AGG(h_v^{(l-1)}, h_u^{(l-1)})) | u \in \mathcal{N}(v)$$

where  $f(\cdot)$  is a function that obtains a new representation  $h_v^l$  for node  $v$  based on its current representation  $h_v^{l-1}$  and the aggregated features from its 1-hop neighbors, i.e.,  $\mathcal{N}(v)$ . The function  $AGG(\cdot)$  represents the specific aggregation mechanism used. Note that the number of layers in a GNN model determines how far it can 'reach' through the network.

GNNs can be trained under two distinct settings, namely, transductive [18, 44, 55, 58] and inductive [12, 27, 36, 47, 48, 52]. In the transductive setting, the GNN learns from both labeled and unlabeled nodes within a fixed graph during training, subsequently predicting the labels for the unlabeled nodes post-training. A significant limitation of this approach is the necessity for retraining the models when new nodes are added to the graph. Contrarily, the inductive setting has garnered more popularity [1, 46] due to its ability to generalize the learned GNN model to previously unseen nodes, thus obviating the need for the time-consuming retraining step when the graph later accrues additional nodes or even subgraphs. This feature significantly augments the practicality of graph data analytics in real-world scenarios. Therefore in this study, *our focus is solely on the inductive settings*, delving specifically into four commonly used inductive GNN architectures: GAT [36], GCN [18], GIN [47], and GraphSAGE [12].

**Graph Convolutional Network (GCN).** GCN [18] updates each node's features by aggregating features from its neighbors and itself. The layer-wise propagation rule for a GCN can be written as:

$$h_v^l = \sigma(W^{(l-1)} \cdot MeanAgg(\{h_u^{(l-1)} : u \in \mathcal{N}(v) \cup \{v\}\}))$$

where  $W$  is a learnable weight matrix,  $\sigma$  is a non-linear activation function, and  $MeanAgg$  calculates the mean of the feature vectors of node  $v$  and its 1-hop neighbors  $\mathcal{N}(v)$ .

**Graph Attention Network (GAT).** GAT [36] computes attention coefficients that indicate the importance of each neighbor's information. The attention-based aggregation in GAT is represented as follows where  $W$  is a trainable weight

matrix,  $\sigma$  is an activation function, and  $\alpha_{vu}$  is the attention coefficient indicating how much attention node  $v$  should pay to node  $u$  during aggregation:

$$h_v^l = \sigma\left(\sum_{u \in \mathcal{N}(v)} \alpha_{vu}^{(l-1)} W^{(l-1)} h_u^{(l-1)}\right)$$

**GraphSAGE** GraphSAGE [12] aims to generate embeddings by sampling and aggregating features from a node's neighbors. With commonly used mean aggregation as an example, the aggregated information for node  $v$  is computed as follows where  $W$  is the weight matrix and  $\sigma$  is the activation function:

$$h_v^l = \sigma(W^{l-1} \cdot CONCAT(h_v^{l-1}, MeanAgg(h_u^{l-1} : u \in \mathcal{N}(v))))$$

**Graph Isomorphism Network (GIN).** GIN [47] uses a parametrized aggregation function that can capture the graph structure by considering both the node itself and its neighbors. The update rule for GIN is defined as follows where  $\varepsilon$  is a learnable parameter and  $MLP$  is a multi-layer perceptron:

$$h_v^l = MLP^{(l-1)}((1 + \varepsilon_v^{(l-1)}) \cdot h_v^{(l-1)} + \sum_{u \in \mathcal{N}(v)} h_u^{(l-1)})$$

## 3 Attack Methodology

### 3.1 Threat Model

**Graph Structure and GNN Specification.** In our setting, a service provider possesses a private graph where nodes represent entities they wish to classify and edges between these nodes capture their relationships or interactions. Crucially, only the service provider can access the full adjacency matrix but individual nodes can view/update their own set of connected nodes. The node features encompass both attributes and actions carried out by the user (owner of the node) on the service platform. The users can also modify their nodes.

The setting outlined above mirrors many practical application contexts of GNN, such as social networks, recommendation systems [4, 15, 43, 49], and intrusion detection systems [1]. For instance, consider a GNN-based recommendation system where the users have access to their personal profiles only and cannot see the entire network.

Following the inductive approach [12, 36, 47], the GNN model is first trained on a foundational graph populated with labeled users (the training phase). It is then subsequently utilized on the continually evolving graph (the inference phase). It's crucial to highlight that all nodes, including those controlled by the adversary, possess only black-box access to the GNN model [13, 14]. The model conducts inference based on the features of the user's node and provides them with the classification output and prediction probabilities (node posterior). Unlike the approaches in [13, 42] which assume universal access to the posterior of all nodes, our model restricts such

Attack	Node Posteriors	Attacker's Knowledge			Shadow Dataset	Attacker's Capability
		Node Features	Partial Graph			
Link Stealing Attack (LSA) [13]	All	All	Yes*	Yes*	Query GNN model on all node features	
LinkTeller Attack (LTA) [42]	All	All	No	No	Query GNN model on all node features	
Our proposed attacks (SIM and INF)	Auxiliary Nodes	Auxiliary Nodes	No	No	Create/modify auxiliary nodes and their edges	

\* indicates knowledge assumptions applicable to some variations of the attack

Table 1: Comparison of Threat Model between Edge Inference Attacks

access to represent a more practical scenario. This limited knowledge, particularly, the absence of the target node’s posterior information, complicates the adversary’s task of identifying its neighbors. **Adversary’s Goal.** The adversary aims to infer the edges of a particular node, which we call the *target node* ( $t$ ). The adversary also defines a *candidate set* ( $C$ ) including the nodes for which the adversary aims to identify whether there is an edge between them and the target node.

**Adversary’s Capability.** In our envisioned scenario, the adversary operates as users within the graph. The service provider is assumed to be honest. The adversary performs an edge inference attack aided by the following capabilities:

- ◆ Introduce new nodes to graph by, e.g., creating new accounts, which we denote as the set of *auxiliary nodes* ( $A$ ).
- ◆ Establish new edges from auxiliary nodes in  $A$  to the target node  $t$  by, e.g., following the account owned by the target node or creating relationships.
- ◆ Alter the features of nodes in  $A$  by, e.g., profile update.
- ◆ Query the GNN model for predictions on the nodes in  $A$ .

All the capabilities listed above are trivial extensions of the assumptions we made regarding the graph structure and GNN specifications. Therefore, they represent the minimal set of abilities a realistic adversary would possess. What’s more, these assumptions have been routinely employed by prior node injection attacks [3, 33, 38, 59, 60]. We provide a comparison of our threat model with prior research [13, 42] in Table 1. Clearly, our threat model imposes the most stringent restrictions on the adversary to uncover the real privacy threats for GNNs in practical applications.

### Algorithm 1 General Pipeline of Our Attacks

**Input:** GNN model  $GNN(\cdot)$ , Target node  $t$ , Candidate node set  $C$ , estimated degree of target node  $\hat{d}$ , Attack method  $AttackMethod()$

**Output:** Res: a boolean vector for nodes in the candidate set, indicating the presence of edge between  $t$  and each  $c \in C$

```

1: for each node  $c \in C$  do
2:    $LPS[c] \leftarrow AttackMethod(GNN, t, c)$ 
3: end for
4:  $threshold \leftarrow (\hat{d} + 1)$ -th largest value in  $LPS$ 
5:  $Res \leftarrow [True \text{ if } LPS[c] > threshold \text{ else False for } c \in C]$ 
6: return  $Res$ 

```

## 3.2 Proposed Attacks

The adversary in our attacks participates in the graph by inserting auxiliary nodes aiming to uncover the private edges of the target node by analyzing model’s prediction for their own nodes only.

**Key Intuitions.** Our attack leverages the message aggregation process inherent in GNNs. Within GNNs, each node accumulates information from its adjacent nodes to build its ultimate representation. Hence, the key intuition we exploit in our attacks’ methodology is that by scrutinizing the posterior of a node, we can infer private information about the nodes directly connected to it. When two nodes  $v$  and  $u$  are connected, the information exchange is bidirectional. On one hand,  $v$  integrates information from  $u$  through message aggregation, making it feasible to infer  $u$ ’s private characteristics via observations on  $v$ . On the flip side,  $v$ ’s existence as a neighboring node alters  $u$ ’s posterior. As a result, an intriguing and viable approach for privacy inference is to analyze the changes in  $u$ ’s posterior prompted by its relationship with  $v$ .

In our attack framework, the adversary seeks to infer the existence of an edge between the target node  $t$  and a candidate node  $c \in C$  by scrutinizing the model’s predictions for the auxiliary nodes ( $A$ ). Specifically, the adversary begins by introducing auxiliary nodes  $A$  in the graph and then forming edges between these nodes and the node pair under investigation. During the inference phase, the adversary queries the GNN model to obtain the prediction probability vectors of the nodes in  $A$ , subsequently utilizing them to infer the relationships between the target node and the candidate nodes. This procedure is illustrated in Figure 1. The attack is considered successful if the attacker accurately identifies nodes from the candidate set that are connected to the target node.



Figure 2: How adversary performs GNNBleed.  $t$ ,  $c$ , and  $a_n$  represents the target node, the candidate set, and the auxiliary nodes respectively. Black dashed lines represent existing edges within the graph, concealed from the adversary’s knowledge, and red lines indicate edges introduced by the adversary.

Our key intuitions lead to the design of multiple attacks, all adhering to the same pipeline depicted in Algorithm 1. For each pair of target node and candidate node, the adversary computes a Link Possibility Score (LPS). Notably, distinct attacks employ varied methods to calculate LPS. Since our attack is unsupervised, in order to establish tangible predic-



tions, the adversary need to select a threshold to determine which scores should be labeled as connected. Inspired by the concept of density belief in *LTA* [42], we utilize the concept that the adversary has an *estimated degree* of the target node, denoted as  $\hat{d}$ , which could deviate from the target node’s true degree  $d$ . During the attack, adversary classifies the top- $\hat{d}$  nodes with the peak LPS values as being connected to the target node. Additionally, if the LPS of a node is zero, we exclude it from consideration. The availability of the degree of the target node fluctuates across various scenarios. For instance, in a social network, the degree of the target node can be determined by the count of followers and followings, which is typically public. However, in certain contexts, the degree information might not be available to the adversary. Therefore, in our experiments, we employed different  $\hat{d}$  values to demonstrate the robustness of our attack.

We have formulated several attacks, broadly divided into two categories: (1) similarity-based edge inference attacks and (2) influence-based edge inference attacks.

### 3.2.1 Similarity-based Edge Inference Attack

The foundational concept behind this attack method relies on the notion that in GNN each node aggregates information from its neighbors to construct its final representation (i.e. posterior). Thus, a node’s posterior is shaped by two elements: (1) its own features and (2) its neighbors’ features. In a situation where two distinct nodes possess identical features, any disparities in their posteriors can only be attributed to differences in their respective neighboring nodes. This leads to a pivotal insight: the more similar the posterior of two nodes with identical features are, the closer the resemblance in their respective neighborhoods. A potential reason the neighborhoods resemble each other is that they are identical. In fact, in graphs devoid of numerous similar subgraphs or neighborhoods, this is the most likely explanation. Thus the high similarity of two nodes’ neighborhoods suggests that they are close to each other. Based on the above intuition, our attack design inserts two identical auxiliary nodes connected to the target and candidate nodes, respectively. If, later on, we observe that their posteriors are similar, we infer that an edge exists between the target and candidate nodes, bringing the inserted nodes closer together. Alternatively, if the posteriors differ, it suggests that the target and candidate nodes aren’t directly connected. We outline the details of the attack below.

**Similarity Attack (SIM).** In this attack, we introduce two auxiliary nodes, i.e.,  $A = \{a_1, a_2\}$ , each possessing identical features. Next, we connect  $a_1$  and  $a_2$  to the victim node  $t$  and a candidate node  $c$ , respectively, as depicted in Figure 2a. Based on our previous discussion, we compute the similarity between the posteriors of nodes  $a_1$  and  $a_2$  and use the similarity as the *LPS* for inferring the presence of an edge. We compute distance using one of the 8 prevalent distance met-

rics: Canberra, Manhattan, and Square-Euclidean distance following [13] and subtract the distance from 1 to get the similarity. For further details regarding our algorithm, refer to Algorithm 2.

---

#### Algorithm 2 Similarity Attack (SIM)

---

**Input:** GNN API  $GNN(\cdot)$  ▷ It accepts a node and returns a prediction for it.  
target node  $t$ , candidate node  $c$   
**Output:** LPS, which quantifies the likelihood that  $t$  and  $c$  are connected  
1:  $G' \leftarrow$  add two auxiliary nodes  $a_1$  and  $a_2$  to the original graph  $G$ , and establishing edges  $(t, a_1)$  and  $(c, a_2)$ , respectively.  
2:  $p_{a_1}, p_{a_2} \leftarrow GNN(a_1), GNN(a_2)$   
3:  $LPS \leftarrow 1 - distance(p_{a_1}, p_{a_2})$   
4: **return** LPS

---

**Shortcomings.** Similarity-based attacks rely on the strong assumption that directly connected nodes draw information from similar neighborhoods and from one another, hence the posterior distributions for directly connected nodes are expected to be highly similar. However, a pair of nodes from the same neighborhood that are not directly connected should exhibit high similarity in the posterior as well. Therefore, it becomes challenging for the attacker to differentiate between nodes directly connected to the target node and nodes that aren’t connected but are in the same neighborhood as the target node.

### 3.2.2 Influence-based Edge Inference Attacks

Influence-based attacks operate by examining how alterations to the features of a particular node impact the posterior of other nodes. To elaborate, let’s consider two auxiliary nodes  $u$  and  $v$  such that the adversary perturbs  $u$  and observes the change in the posterior of  $v$ . The *influence* of  $u$  on  $v$  is defined as  $I(v, u) = \frac{norm(p'_v - p_v)}{\alpha}$  where  $p_v$  and  $p'_v$  are the posteriors of  $v$  before and after the perturbation on  $u$  by a factor of  $\alpha$  (perturbing  $y$  by a factor of  $\alpha$  changes it to  $(1 - \alpha)y$ ). Let,  $P = (u, x, \dots, v)$  be the shortest path connecting  $u$  and  $v$ . The influence of  $u$  on  $v$ ,  $I(v, u)$ , depends on two essential factors: (1) the distance between  $u$  and  $v$ , i.e. the length of  $P$  and (2) the weight of  $u$  when aggregating on the subsequent node  $x$  along the path  $P$ . If  $u$  and  $v$  are close to each other,  $I(v, u)$  would be high, because information travels more directly between them. Conversely, if they are distant,  $I(v, u)$  would be low. In other words, the distance between  $u$  and  $v$  is related to the magnitude of  $I(v, u)$ . In our first influence attack, we utilize the above factor to determine the existence of an edge between a target node and a candidate node. Let’s consider  $a_1$  and  $a_2$  in place of  $u$  and  $v$ . From Figure 2, we can deduce the following: if there’s an edge between  $t$  and  $c$ , the distance between  $a_1$  and  $a_2$  is 3. If there’s no edge, the distance is greater than 3. The former case would result in a higher influence  $I(a_2, a_1)$  than the latter case. Therefore, observing the value of  $I(a_2, a_1)$  can aid the adversary in predicting the existence of an edge between  $t$  and  $c$ . With this in mind, we design our first influence-based attack as follows.

**Influence Attack 1 (INF1).** This attack begins by adding two auxiliary nodes, i.e.,  $A = \{a_1, a_2\}$ , which are connected to  $t$  and  $c$  respectively, as depicted in Figure 2a. Following this, the adversary can obtain the model’s predictions for  $a_1$  and  $a_2$ , denoted as  $p_{a_1}$  and  $p_{a_2}$ , respectively. The adversary then perturb the node feature of  $a_1$  with a perturbation factor of  $\alpha$ , such that  $feature_{a_1}' = (1 - \alpha)feature_{a_1}$ , where  $feature_{a_1}'$  represents the updated feature of the node. We set  $\alpha = 0.0001$  to minimize the feature change. The same  $\alpha$  is employed for all node pairs in the attack, rendering the specific value of  $\alpha$  inconsequential to the attack outcome. After this step, the attacker can get a new prediction for node  $a_1$ , called  $p_{a_1}'$ . The influence of  $a_1$  on  $a_2$  can then be calculated as  $I(a_2, a_1) = \frac{norm(p_{a_1}' - p_{a_1})}{\alpha}$ . Afterward, the influence score  $I(a_2, a_1)$  is used as the *LPS* for inferring the presence of an edge based on our prior discussion. The implementation of this attack is demonstrated in Algorithm 3.

---

### Algorithm 3 Influence Attack 1 (INF1)

---

**Input:** GNN API  $GNN(\cdot)$  ▷ It accepts a node and returns a prediction for it.  
target node  $t$ , candidate node  $c$   
**Output:** *LPS*, which quantifies the likelihood that  $t$  and  $c$  are connected  
1:  $G' \leftarrow G$  update the API internal graph with modifications as follows:  
2: – Add nodes  $a_1$  and  $a_2$ .  
3: – Establish edges:  $(t, a_1)$  and  $(c, a_2)$ .  
4:  $p_{a_2} \leftarrow GNN(a_2)$   
5:  $G' \leftarrow$  perturb the feature of  $a_1$   
6:  $p_{a_1}' \leftarrow GNN(a_1)$   
7:  $LPS \leftarrow norm(p_{a_1}' - p_{a_1})$   
8: **return** *LPS*

---

**Shortcomings of INF1 and Inclusion of an Anchor Auxiliary Node.** *INF1* exhibits a clear limitation - the influence  $I(a_2, a_1)$  does not exclusively hinge on the distance between the target node  $t$  and the candidate node  $c$ . The weight of the node  $a_2$ , when aggregating features from the neighbors of  $c$ , significantly affects the value of  $I(a_2, a_1)$ . The weight is modulated by factors such as the degree of node  $c$ , the exact value of which is not known to the adversary. Because of this,  $I(a_2, a_1)$  might be low for certain pairs of connected  $t$  and  $c$  making it challenging for the adversary to determine an optimal threshold. Put simply, relying exclusively on  $I(a_2, a_1)$  for edge identification could lead to numerous incorrect predictions. Therefore, we need to consider an edge likelihood estimation scheme that is not dependent on the aggregation weight of  $a_2$  on  $c$ .

To address this problem, we introduce a third auxiliary node, termed the *anchor node*,  $a_{anchor}$ , which shares identical features with  $a_1$  and  $a_2$  and is directly connected to the candidate node  $c$  (depicted in Figure 2b). The key insight is that, given the identical features of  $a_2$  and  $a_{anchor}$ , they are expected to have the same aggregation weight on  $c$ . Moreover, the influence of  $a_2$  on  $a_{anchor}$  exclusively depends on the aggregation weight of  $a_2$  on  $c$ . Thus, the value of  $I(a_{anchor}, a_2)$  acts as an indicator of the  $a_2$ ’s aggregation weight on  $c$  for the adversary. Another important observation is that, although the precise value of  $I(a_1, a_2)$  hinges on the aggregation weight of  $a_2$  on

$c$ , the closeness between  $I(a_1, a_2)$  and  $I(a_{anchor}, a_2)$  is exclusively dependent on whether  $t$  and  $c$  are directly connected. Put another way, when  $t$  and  $c$  are connected, the influence score resulting from a feature perturbation in  $a_2$  would be similar for both  $a_1$  and  $a_{anchor}$  regardless of factors affecting aggregation weight of  $a_2$  on  $c$ . However, in the absence of a connection between  $t$  and  $c$ ,  $I(a_1, a_2)$  would be noticeably smaller than  $I(a_{anchor}, a_2)$ . This difference can help us ascertain whether there’s a connection between  $t$  and  $c$ . Similar to the relationship between  $I(a_1, a_2)$  and  $I(a_{anchor}, a_2)$ , we can investigate the posterior changes of  $a_1$  and  $a_{anchor}$ ,  $(p_{a_1}' - p_{a_1})$  and  $(p_{a_{anchor}}' - p_{a_{anchor}})$  respectively, to predict the existence of an edge between  $t$  and  $c$ . Therefore, we introduce two new versions of the influence-based attack: influence attack 2 (*INF2*) and influence attack 3 (*INF3*). The former investigates the distance between  $(p_{a_1}' - p_{a_1})$  and  $(p_{a_{anchor}}' - p_{a_{anchor}})$  while the latter investigates the ratio of  $I(a_1, a_2)$  and  $I(a_{anchor}, a_2)$  to determine whether  $t$  and  $c$  are directly connected.

**Influence Attack 2 (INF2).** In this attack approach, we inject three auxiliary nodes, i.e.,  $A = \{a_1, a_2, a_{anchor}\}$ , each initialized with identical features, and establish three edges  $(t, a_1)$ ,  $(c, a_2)$ , and  $(c, a_{anchor})$ , as depicted in Figure 2b. Following this arrangement, the adversary is capable of obtaining the model’s predictions for these nodes, designated as  $p_{a_1}$ ,  $p_{a_2}$  and  $p_{a_{anchor}}$ . To proceed further, the adversary reassigns the node feature of  $a_2$  by perturbation with a factor of  $\alpha$ , leading to  $feature_{a_2}' = (1 - \alpha)feature_{a_2}$ , where  $feature_{a_2}'$  stands for the refreshed feature of the node. Following that, we measure the impact of the perturbation of  $a_2$  on posterior changes of  $a_1$  and  $a_{anchor}$ ,  $(p_{a_1}' - p_{a_1})$  and  $(p_{a_{anchor}}' - p_{a_{anchor}})$  respectively, and calculate the distance between these posterior change vectors,  $distance(p_{a_1}' - p_{a_1}, p_{a_{anchor}}' - p_{a_{anchor}})$ . Following our discussion in the preceding paragraph, a small distance implies the existence of an edge between  $t$  and  $c$ , whereas a high distance implies no edge. Thus, in *INF2*, we define the *LPS* as 1 minus this distance. In the experiment, we deploy eight distance metrics: Cosine, Euclidean, Correlation, Chebyshev, Braycurtis, Canberra, Manhattan, and Square-euclidean distances to evaluate similarity. The specific implementation of this attack is articulated in Algorithm 4.

---

### Algorithm 4 Influence Attack 2 (INF2)

---

**Input:** GNN API  $GNN(\cdot)$  ▷ It accepts a node and returns a prediction for it.  
target node  $t$ , candidate node  $c$   
**Output:** *LPS*, which quantifies the likelihood that  $t$  and  $c$  are connected  
1:  $G' \leftarrow G$  update the API internal graph with modifications as follows:  
2: – Add nodes  $a_1$ ,  $a_2$ , and  $a_{anchor}$ .  
3: – Establish edges:  $(t, a_1)$ ,  $(c, a_2)$ , and  $(c, a_{anchor})$ .  
4:  $p_{a_1}, p_{a_{anchor}} \leftarrow GNN(a_1), GNN(a_{anchor})$   
5:  $G' \leftarrow G'$  perturb the feature of  $a_2$   
6:  $p_{a_1}', p_{a_{anchor}}' \leftarrow GNN(a_1), GNN(a_{anchor})$   
7:  $LPS \leftarrow 1 - distance(p_{a_1}' - p_{a_1}, p_{a_{anchor}}' - p_{a_{anchor}})$   
8: **return** *LPS*

---

**Influence Attack 3 (INF3).** The setup phases of this attack strategy mirror those of *INF2* – we insert 3 auxiliary nodes including an anchor one  $\{a_1, a_2, a_{anchor}\}$  and perturb

the feature of  $a_2$  following  $feature'_{a_2} = (1 - \alpha)feature_{a_2}$ . However, in *INF3*, we use the relationship between  $I(a_1, a_2)$  and  $I(a_{anchor}, a_2)$  to predict the existence of an edge between  $t$  and  $c$ . Since  $a_{anchor}$  is a 2-hop neighbor of  $a_2$  and the distance between  $a_1$  and  $a_2$  is at least 3, it is expected that  $I(a_{anchor}, a_2)$  exceeds  $I(a_1, a_2)$  serving as an upper bound for the latter. Because of this, we compute the ratio of  $I(a_1, a_2)$  and  $I(a_{anchor}, a_2)$ , and use the resulting fraction as a likelihood that  $t$  and  $c$  are connected. If the ratio approaches 1, it suggests there’s a high likelihood of an edge existing between  $t$  and  $c$ . On the other hand, if the value is near 0, it indicates a low likelihood of such an edge. The implementation of this attack is demonstrated in Algorithm 5.

---

**Algorithm 5** Influence Attack 3 (INF3)

---

**Input:** GNN API  $GNN(\cdot)$  ▷ It accepts a node and returns a prediction for it.  
target node  $t$ , candidate node  $c$   
**Output:** LPS, which quantifies the likelihood that  $t$  and  $c$  are connected  
1:  $G' \leftarrow G$  update the API internal graph with modifications as follows:  
2: – Add nodes  $a_1, a_2, a_{anchor}$ .  
3: – Establish edges:  $(t, a_1), (c, a_2)$  and  $(c, a_{anchor})$ .  
4:  $p_{a_1}, p_{a_{anchor}} \leftarrow GNN(a_1), GNN(a_{anchor})$   
5:  $G'^l \leftarrow G'$  perturb the feature of  $a_2$   
6:  $p'_{a_1}, p'_{a_{anchor}} \leftarrow GNN(a_1), GNN(a_{anchor})$   
7:  $LPS \leftarrow I(a_1, a_2) / I(a_{anchor}, a_2)$   
8: **return** LPS

---

## 4 Evaluation

### 4.1 Datasets

We evaluate our attacks along with the state-of-the-art attacks on 7 datasets: Flickr [52], LastFMAsia [29], and Twitch-{DE, EN, FR, PT, RU} [28].

*Twitch* dataset contains six separate graphs, each reflecting data from a distinct country. Users represent nodes while edges represent follower connections. Node features correspond to the embeddings of games played by users. The dimension of the features remains the same across different graphs. The task is binary classification to predict whether a user streams mature content. This dataset is structured for transfer learning, meaning the model is trained on one country’s graph and then applied to the graphs of other countries. *Flickr* is an image relationship dataset where each node represents an image. The features of each node are characterized by bag-of-words models derived from their descriptions, while the edges between them indicate common attributes shared by the images. The task is to classify the images into one of the 7 classes.

*LastFmAsia* is a social network graph where nodes symbolize LastFM users from Asia and the edges represent friendships between these users. The node features are extracted based on the artists liked by the users. The task in this dataset is to predict the users’ nationality.

For the Twitch dataset, we train the GNN model on the Twitch-ES dataset and then apply it to the other five countries’ graphs.

For both the Flickr and LastFmAsia datasets, we randomly partition the data into training, validation, and test sets using ratios of 70%, 15%, and 15%, respectively. During training, the model accesses the subgraph composed of only the training nodes. However, during testing and validation, predictions are made based on the entirety of the graph. More details of the datasets can be found in Appendix A.2.

### 4.2 Models

We evaluate the attacks on four types of GNN models- GAT [36], GCN [18], GIN [47], and GraphSAGE [12], each with a 4-layer architecture. Note that, for GraphSAGE [12], we disable the neighborhood sampling during inference.

Our choice for a 4-layer architecture stems from the pivotal role the number of layers, represented as  $l$ , plays in GNNs. The parameter  $l$  specifically sets the cap for how many layers of deep information can traverse within the GNN. Consequently, any alterations to the feature of a node will resonate across its  $l$ -hop neighbors. To illustrate, consider two nodes,  $v$  and  $u$ , with an edge in between. Our attacks introduce two new nodes,  $a_1$  and  $a_2$ , linked to  $v$  and  $u$ , respectively, forming edges  $(a_1, v)$  and  $(a_2, u)$ , resulting in  $a_1$  and  $a_2$ ’s distance to be 3. This suggests that our influence attacks would be efficacious on a model with at least 3 layers, and would be ineffective on models with less than 3 layers. To maintain a balanced evaluation, we have opted to utilize GNNs with four layers. Previous attacks, such as those by He et al. [13] and Wu et al. [42], primarily focus on 2-layer and 3-layer models, arguing that adding more layers may degrade the performance of the trained model. However, recent research underscores that GNN models with up to 5 layers are useful which indicates the potential advantages of deeper GNN models [21, 22, 51]. Considering the depth required for effective information propagation in GNNs, it’s logical for us to explore models with a depth beyond three layers.

### 4.3 Experiment Setup

**Metrics.** We employ precision, recall, F1-score, and ROC-AUC to evaluate the attacks. Precision is indicative of the ratio of correctly identified edges to all edges predicted by the adversary. Recall measures the proportion of actual edges that were successfully uncovered by the adversary from the pool of real edges. The F1 score is a harmonic mean of precision and recall, providing a balanced metric for evaluating classification model performance. Additionally, we employ the AUC (area under the ROC curve), a threshold-independent metric for binary classification, aligning with prior works [13, 42]. See Appendix A.1 for details of the metrics.

**Baseline Attacks.** We compare our attack with two state-of-the-art attacks as described below:

*Link Stealing Attack (LSA)* [13]: Based on varying assumptions about what the adversary knows, LSA outlines multiple

attack strategies for transductive GNNs. We use *LSA-0* as the baseline as it closely aligns with the adversary capabilities in our attack, where the attacker gathers statistics for edge inference solely based on the model output. *LSA-0* infers edges based on the similarity between posteriors of two nodes. We adapt *LSA* to the inductive setting by computing the similarity between the target node and the nodes within the candidate set. We’ve opted for the correlation distance between node posteriors for link inference, following the best practice. *LinkTeller Attack (LTA)* [42]: *LTA* discerns links by analyzing the influence one node exerts on others. In contrast to our attacks where the adversary can modify only their own nodes, *LTA* assumes that the adversary has access to, and can manipulate the features of all nodes in the graph. Within *LTA*, the adversary leverages the influence each node imposes on every other node to identify existing edges.

For comparative analysis, the threshold in both baseline attacks is set to label the top  $k$  node pairs as connected—ranked by their respective metrics, i.e., similarity in *LSA* and influence score in *LTA*, where  $k$  is the adversary’s estimate of the target node’s degree.

**Target Node and Candidate Set Selection.** For each dataset, we randomly choose 100 nodes as target nodes and all results demonstrated in the later sections represent the average across these nodes. For each target node, we restrict the candidate set members to only its 2-hop neighbors (negative samples) and the nodes directly connected to it (positive samples). Prior research, *LSA* and *LTA* [13,42], opted to randomly select node pairs and infer the edges between them. However, random sampling often produces negative samples that are notably remote from the target node, consequently making it relatively straightforward for the adversary to distinguish the nodes directly connected to the target from the ones that are far apart. In contrast, restricting the candidate sets to nodes that have a distance of at most two from the target node allows us to evaluate the performance of the inference attacks more effectively. Additionally, the way we select the candidate set is more practical and reflective of real-world situations. For example, in the realm of social networks, it’s plausible for an adversary’s candidate set to predominantly comprise nodes from the same local community or neighborhood.

**Target Node Degree Estimation by the Adversary.** In our attack strategy, estimated degrees of the target node serves as the basis for establishing thresholds. While applicable in contexts like social networks, where follower counts are public, this strategy encounters challenges where such information is inaccessible. In these scenarios, adversaries may possess inaccurately estimated degrees, and subsequently, the efficacy of the attack can vary. For a comprehensive evaluation, given the ground truth degree  $d$ , we incorporate three approximations:  $0.8d$ ,  $d$ , and  $1.2d$ . It’s important to highlight that multiplying the degree by 0.8 or 1.2 doesn’t always result in an integer. Therefore, for underestimation, we apply  $\hat{d} = \lfloor 0.8d \rfloor$  to round down to the nearest whole number. Conversely, for overesti-

mation, we implement  $\hat{d} = \lceil 1.2d \rceil$ , rounding up to provide a figure slightly above the actual degree. The purpose of this exercise is to analyze the effect of these variances, both in overestimating and underestimating the actual node degree, on our attack’s precision and recall.

**Target Node Degree Range.** Adversaries often concentrate on nodes across different degree distributions, as outlined in [42]. Consequently, we investigate three distinct node subsets based on their degree of connectivity: those with low, unconstrained, and high degrees. Owing to space constraints, we delineate the specific criteria for these categorizations in Appendix B.2.

**Feature Selection for Auxiliary Nodes (A).** We consider five distinct strategies to set the features of auxiliary nodes:

- ◆ *Random:* The feature is picked randomly.
- ◆ *Target Node Duplication:* The feature is the same as the target node.
- ◆ *Mean:* The mean of each feature is computed across all nodes and the resulting feature vector is assigned to  $A$ .
- ◆ *Dataset Typical:* The feature of the node having the shortest Euclidean distance to the mean is adopted.
- ◆ *Median:* The feature is determined by computing the median of each feature across all existing nodes.

Note that, except for the first, all node feature selection strategies outlined above assume extra adversarial knowledge. Nonetheless, the variation in node feature selection strategies enables us to identify the strongest version of our attacks, highlighting the potential extent of privacy breaches.

## 4.4 Attack Performances

We evaluate GNNBleed in three steps: we first compare its performance with the baseline attacks. Next, we assess GNNBleed’s strength across nodes of varying degrees and test its robustness against inaccurate degree assumptions made by the adversary. Finally, we examine how the chosen features for nodes in  $A$  influence attack effectiveness.

### 4.4.1 Comparison of Attack Methods

The F1 scores for all attack methods are illustrated in Figure 3 and the AUCs are reported in Table 2. These F1 scores are computed under the assumption that the adversary has comprehensive knowledge of node degrees (i.e., the estimated degree  $\hat{d}$  is equal to the true degree  $d$ ). This is deemed a fair setting, as we establish the threshold for all attacks in a uniform manner. Features of nodes in  $A$  are sampled randomly, and the degree of the target node remains unconstrained. For *SIM* and *INF2*, in which we require using distance metrics, we present their results only with the best-performing metrics, correlation distance for *SIM* and Bray–Curtis distance for *INF2*, due to space limitations. For comprehensive results, please refer to Appendix B.1.



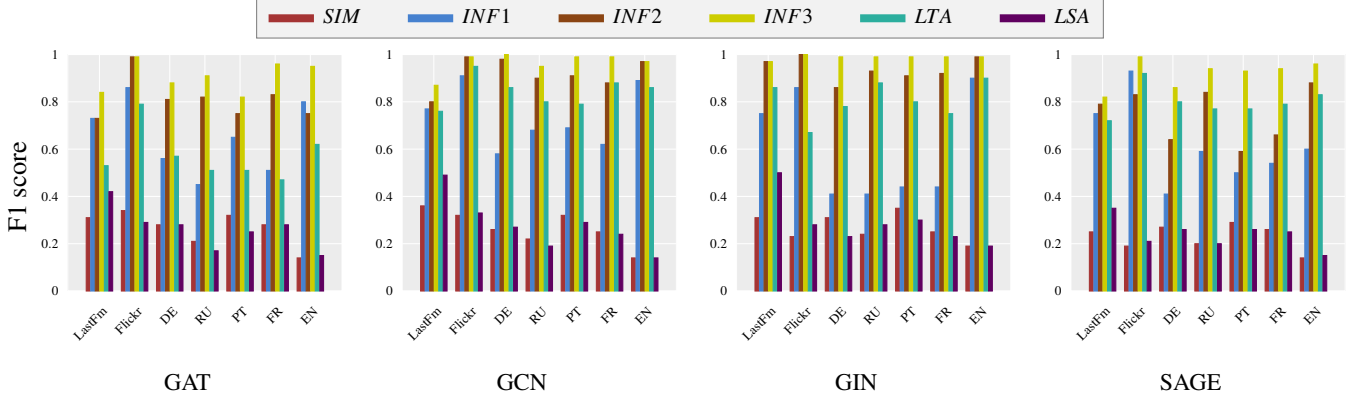


Figure 3: Comparative Analysis of Attack Performances: The graph illustrates the average F1 score from all attacks, computed across seven datasets and four types of GNN models. Each score is averaged from attacks on 100 target nodes. The datasets are represented on the x-axis, while the y-axis depicts the F1 score.

Table 2: AUC Metrics for Various Attacks: Each row signifies a distinct dataset, while column groups illustrate types of attacks against different GNN models.

Dataset	SIM				INF1				INF2				INF3				LTA				LSA			
	GCN	SAGE	GAT	GIN	GCN	SAGE	GAT	GIN	GCN	SAGE	GAT	GIN	GCN	SAGE	GAT	GIN	GCN	SAGE	GAT	GIN	GCN	SAGE	GAT	GIN
LastfmAsia	0.81	0.76	0.79	0.72	0.81	0.76	0.79	0.77	0.98	0.98	0.98	0.97	0.99	0.99	0.99	0.97	0.98	0.92	0.86	0.91	0.91	0.91	0.83	
Flickr	0.73	0.64	0.74	0.67	0.98	0.97	0.97	0.95	0.99	0.99	0.95	0.99	0.99	0.99	0.99	0.99	0.99	0.94	0.94	0.76	0.64	0.74	0.68	
Twitch-EN	0.73	0.64	0.74	0.59	0.98	0.97	0.97	0.90	0.99	0.99	0.95	0.99	0.99	0.99	0.99	0.99	0.99	0.94	0.90	0.76	0.64	0.74	0.58	
Twitch-DE	0.58	0.58	0.58	0.59	0.91	0.64	0.82	0.84	0.99	0.93	0.94	0.99	0.99	0.96	0.97	0.98	0.93	0.76	0.91	0.57	0.59	0.57	0.69	
Twitch-FR	0.73	0.64	0.74	0.65	0.98	0.97	0.97	0.70	0.99	0.99	0.95	0.99	0.99	0.99	0.99	0.99	0.99	0.94	0.89	0.76	0.64	0.74	0.65	
Twitch-PT	0.73	0.64	0.74	0.57	0.98	0.97	0.97	0.71	0.99	0.99	0.95	0.99	0.99	0.99	0.99	0.99	0.99	0.94	0.95	0.76	0.64	0.74	0.66	
Twitch-RU	0.58	0.59	0.59	0.57	0.91	0.77	0.79	0.71	0.99	0.96	0.95	0.99	0.99	0.99	0.99	0.99	0.96	0.79	0.95	0.59	0.61	0.59	0.66	

Reviewing the results, similarity-based attacks, including the *LSA* and our proposed *SIM* attack, consistently underperform across multiple test scenarios. It is a finding we deem to be quite logical. The foundational assumption behind these attacks is that nodes directly connected would draw information from similar neighborhoods and from one another, hence anticipating a heightened similarity in the posterior distributions for directly connected nodes. *Nevertheless, this principle fails in our experimental context where all nodes are chosen from identical neighborhoods, obfuscating the distinction between nodes that are directly connected and those merely in close proximity.* With respect to *LTA*, while the attack shows impressive results with GCN and GIN (F1 score surpassing 0.8), it demonstrates diminished efficacy against GAT (F1 score drops to approximately 0.5). The outcomes align with our expectations, given that *LTA* overlooks weight in message aggregation. Although it proves effective for some GNNs such as GCN and GraphSage which utilize the basic mean function and assign uniform weight to nodes, it stumbles with GIN and GAT that implement advanced aggregation methods and assign considerably varied weights to each node. While *INF1* exhibits superiority over similarity-based attacks, its efficacy generally falls short when compared to *LTA*, despite they share the same idea. This discrepancy is due to the different node distances analyzed. *LTA* accesses model outputs for target and candidate nodes directly, while *INF1* focuses on ANs,

adding two more hops to the message passing path compared to the distance in *LTA*. In GNNs’ message passing, each node modifies the message, causing cumulative alterations. These additional two hops introduce more distortion, complicating the inference task for the adversary. This result highlights the significant challenges inherent in executing influence analysis within the constraints imposed by our scenario.

Our *INF2* attack demonstrates both greater consistency and superior performance when compared to *LTA* and *INF1*. It achieves good performance when evaluated against GCN and GIN (F1 score surpassing 0.8 and AUC surpassing 0.95) and maintains its effectiveness when tested with GAT (F1 score around 0.8 and AUC surpassing 0.95). Importantly, even though the F1 scores of the *INF2* attack aren’t consistently better than *LTA*, the AUC scores exceed the latter in most cases. This suggests that *INF2* possesses superior overall discriminative power. However, it’s worth noting that the way we define the threshold may not fully maximize its potential.

The *INF3* attack consistently outperforms other attacks regardless of the model architecture or dataset. It steadily achieves F1 scores above 0.8, often exceeding 0.9 in multiple instances. Similarly, its AUC score reaches up to 0.99 in a substantial majority of testing scenarios. This robust performance is largely credited to its strategic neutralization of weight impacts. By utilizing an anchor node, the *INF3* attack significantly diminishes the weight’s influence during

Table 3: Performance of *INF3* attack on target nodes with different degree distributions and threshold estimation.

$\hat{d}$	Model	Low Degree		Unconstrained		High Degree	
		Recall	Precision	Recall	Precision	Recall	Precision
$[0.8d]$	GCN	0.686	0.952	0.717	0.966	0.796	0.995
	SAGE	0.686	0.952	0.717	0.966	0.798	0.998
	GAT	0.676	0.940	0.704	0.949	0.783	0.98
	GIN	0.686	0.952	0.717	0.966	0.798	0.998
$d$	GCN	0.966	0.966	0.976	0.976	0.992	0.992
	SAGE	0.966	0.966	0.976	0.976	0.998	0.998
	GAT	0.934	0.934	0.938	0.938	0.966	0.966
	GIN	0.966	0.966	0.976	0.976	0.998	0.998
$\lceil 1.2d \rceil$	GCN	1.0	0.789	1.0	0.801	1.0	0.833
	SAGE	1.0	0.782	1.0	0.795	1.0	0.833
	GAT	0.986	0.771	0.989	0.787	0.998	0.831
	GIN	1.0	0.782	1.0	0.795	1.0	0.833

(a) LastFmAsia

$\hat{d}$	Model	Low Degree		Unconstrained		High Degree	
		Recall	Precision	Recall	Precision	Recall	Precision
$[0.8d]$	GCN	0.757	0.999	0.758	0.999	0.789	0.993
	SAGE	0.757	1.0	0.757	0.999	0.792	0.990
	GAT	0.757	1.0	0.757	0.998	0.785	0.981
	GIN	0.757	1.0	0.758	1.0	0.80	1.0
$d$	GCN	0.999	0.999	0.999	0.999	0.985	0.985
	SAGE	0.996	0.996	0.992	0.992	0.986	0.986
	GAT	0.999	0.999	0.999	0.999	0.979	0.979
	GIN	1.0	1.0	1.0	1.0	1.0	1.0
$\lceil 1.2d \rceil$	GCN	1.0	0.825	1.0	0.829	0.999	0.888
	SAGE	1.0	0.830	1.0	0.839	1.0	0.903
	GAT	1.0	0.825	1.0	0.829	1.0	0.891
	GIN	1.0	1.0	1.0	1.0	1.0	1.0

(b) Flickr

$\hat{d}$	Model	Low Degree		Unconstrained		High Degree	
		Recall	Precision	Recall	Precision	Recall	Precision
$[0.8d]$	GCN	0.730	0.996	0.765	1.0	0.785	1.0
	SAGE	0.730	0.996	0.758	0.992	0.773	0.993
	GAT	0.698	0.952	0.719	0.939	0.733	0.934
	GIN	0.730	0.996	0.765	0.999	0.785	0.999
$d$	GCN	0.997	0.997	0.999	0.999	0.999	0.999
	SAGE	0.959	0.959	0.954	0.954	0.956	0.956
	GAT	0.897	0.897	0.894	0.894	0.901	0.901
	GIN	0.997	0.997	0.999	0.999	0.998	0.998
$\lceil 1.2d \rceil$	GCN	1.0	0.814	1.0	0.823	1.0	0.831
	SAGE	0.972	0.836	0.935	0.867	0.921	0.882
	GAT	0.956	0.794	0.966	0.812	0.969	0.820
	GIN	1.0	0.998	0.999	1.0	0.998	1.0

(c) Twitch-DE

the process, placing principal emphasis on distance as the predominant factor affecting influence. This result demonstrates that, *INF3*'s utilization of anchor node is more effective than *INF2*. The similar AUC scores achieved by both *LTA* and *INF3* when evaluated against models such as GCN provide strong evidence of the effectiveness of our attack. Despite the fact that *LTA* necessitates access to all model outputs and designed specifically for GCN, *INF3* is still able to achieve comparable performance in terms of AUC. This underscores the robustness and competitive nature of our *INF3* attack.

#### 4.4.2 Target Node Degree and Estimated Degree

Table 3 illustrates the efficacy of the *INF3* attack under varying conditions, specifically examining its precision and accuracy across target nodes with different degrees. The experiment further incorporates scenarios where the adversary's estimated degree deviates from the actual degree.

We observe that there is no significant performance change across different node degree distributions, which means the susceptibility of the model to attacks is largely invariant to the heterogeneity of target node connectivity. We attribute this to the degree's impact, which predominantly influences the weighting in message aggregation. However, our *INF3* attack effectively neutralizes the influence of weight, consequently maintaining consistent performance throughout. Further, we observe that with precise degree estimation (where  $\hat{d} = d$ ), *INF3* consistently exhibits high precision and recall. Intriguingly, even when the density estimation deviates, the attack remains robust. This observation aligns with the results in Table 2, where our attack consistently achieves a high AUC, approaching 1.

Table 3 reveals that overestimating target nodes' degrees (using  $\lceil 1.2d \rceil$ ) keeps recall metrics exceedingly high, exceeding 0.99 in most scenarios, underscoring our *INF3* attack's proficiency in uncovering all linked nodes. Intriguingly, the precision demonstrates minimal fluctuation even under suboptimal thresholds, a trend especially prominent in GIN models. Ordinarily, if there's a degree overestimation, the attack will predict more candidate nodes as connected (predicted positive instances) than there are actually connected nodes to the target node (true positive instances). This can lead to an increase in false positive instances, which in turn would decrease precision. However, our proposed attack does not label any node with a zero Link Possibility Score (LPS) as connected even if the total number of predicted connections falls short of the estimated degree. This approach reduces false positives in cases of overestimation and maintains precision.

In the case of underestimating, i.e.,  $[0.8d]$ , precision improves for Twitch-DE and Flickr, while it experiences a slight decline for LastFm, notably when target nodes possess a low or unconstrained degree. This contrast can be attributed to the inherent variability and noise sensitivity when dealing with smaller sample sizes. In contexts where degrees are low, the pool of positive samples shrinks, amplifying the impact of individual errors on the overall precision metric. Essentially, a single misclassification can significantly skew the precision in situations with fewer actual connections. However, this issue diminishes with high-degree cases, where the larger volume of positive samples dilutes the effect of missteps, lending more stability to the precision measurements.

#### 4.4.3 Features of Auxiliary Nodes

The outcomes of the *INF3* attack, taking into account varied selections of auxiliary node features, are shown in Table 4.

Table 4: Performance (F1 score) of the *INF3* Attack with Varied Inserted Node Feature Selection Strategy

Model	Node Feature	LastFmAsia	Flickr	Twitch-DE	Twitch-EN
GCN	Random	0.976	1.0	0.992	0.996
	Typical	0.976	1.0	0.972	0.996
	Duplication	0.976	1.0	0.987	0.996
	Mean	0.936	1.0	0.965	0.996
	Median	0.976	1.0	0.972	0.996
GAT	Random	0.938	1.0	0.899	0.976
	Typical	0.966	1.0	0.981	0.976
	Duplication	0.969	1.0	0.944	0.976
	Mean	0.963	0.999	0.960	0.940
	Median	0.963	0.999	0.979	0.994
SAGE	Random	0.976	1.0	0.969	0.983
	Typical	0.976	1.0	0.973	0.977
	Duplication	0.976	1.0	0.968	0.983
	Mean	0.751	0.992	0.962	0.964
	Median	0.976	0.999	0.967	0.981
GIN	Random	0.976	1.0	1.0	0.996
	Typical	0.976	1.0	1.0	0.996
	Duplication	0.976	1.0	1.0	0.996
	Mean	0.977	1.0	1.0	0.996
	Median	0.976	1.0	1.0	0.996

Due to space constraints, we present attack results for only 4 datasets; comprehensive results are available in Appendix B.3. The results indicate that, despite some variations in attack performance with different node features, the attack remains consistently effective. In our analysis, node features appear not to be a significant determinant of the attack outcome. Specifically, the crux of the *INF3* strategy lies in computing the norm of alterations in the node’s posterior probabilities, quantifying influence. Importantly, even when targeting the GAT model which tailors its weight assignments based on node features, the attack’s performance demonstrates limited variation with different node features. This consistent behavior can be attributed to our approach of using the same features for all auxiliary nodes, thus preserving the relative weight distribution among them.

## 5 Defense

Previous literature has discussed several countermeasures to mitigate privacy attacks against GNNs [16, 30, 42]. A common counterstrategy is *Confidence Masking*, where the model reveals only the top- $k$  confidences, thereby obscuring detailed output [16]. However, by limiting the details accessible from the model’s predictions, users may not gain comprehensive insights, potentially undermining the model’s utility.

More refined countermeasures designed for GNNs have been unveiled through the application of Differential Privacy (DP). For instance, Wu et al. [42] propounded an edge-level DP learning algorithm tailored for GNNs. This approach proposed two strategies to perturb the graph: (1) *EdgeRand*: randomly flipping each entry in the adjacency matrix according to a Bernoulli random variable and (2) *LapGraph*: applying Laplacian mechanism on the entire adjacency matrix while maintaining the overall density. Subsequently, a GNN is trained and inferred on the noise-infused graph. However, a

significant trade-off arises from this privacy-preserving noise infusion, as it inherently impairs the performance of the resulting model. Another avenue for implementing DP resides in infusing noise into the message aggregation. Recent endeavors have proposed privacy-preserving GNN architectures [19, 30] crafted to uphold privacy by adding noise to the output of the aggregation function. While effective for privacy, this innovation presents practical challenges. It necessitates an entirely new GNN architecture, complicating the integration with existing graph-based applications due to high replacement costs and compatibility issues with more advanced GNN models. Given these implications and our focus on widely-adopted GNN architectures, we consider such methods beyond the purview of our current investigation.

Table 5: F1 Score of the *INF3* Attack in the context of Confidence Masking: each row denotes a different model, while each column indicates the number of output probabilities accessible to the adversary.

Model	2	3	4	5	6
GAT	0.922	0.976	0.936	0.933	0.927
GCN	0.976	0.976	0.976	0.976	0.976
GIN	0.976	1.0	0.976	0.976	0.976
SAGE	0.936	0.936	0.976	0.976	0.976

(a) LastFmAsia

Model	2	3	4	5	6
GAT	0.967	0.987	0.988	0.988	0.970
GCN	0.998	0.998	0.998	0.998	0.998
GIN	0.988	0.988	0.988	0.989	1.0
SAGE	0.976	0.976	0.976	0.976	0.976

(b) Flickr

**Confidence Masking.** We vary the parameter  $k$ , representing the top- $k$  highest probabilities that are accessible to the attacker, ranging from 2 to 6. Since the Twitch datasets concern binary classification tasks, this set of experiments is confined to Flickr and LastFmAsia. As displayed in Table 5, limiting the output has no discernible impact on our attack strategies. The result shows that partial output appears to be sufficient for our *INF3* attack.

**Adding Noise to the Graph with Differential Privacy (DP).** We employed EdgeRand and LapGraph [42] to introduce perturbations to the graph. For EdgeRand, we varied the privacy budget  $\epsilon$  between 5 and 10. And for LapGraph, we varied the privacy budget  $\epsilon$  between 2 and 10. We then trained a variety of model architectures using the perturbed graph, subsequently evaluating the efficacy of our attack against these models. The attack performance on the LastfmAsia dataset is illustrated in Fig. 4, with model utility depicted in Fig. 5. In Fig. 4, we present a comparative evaluation of our *INF3* attack and *LTA*, for a range of privacy budget parameter  $\epsilon$  values. Meanwhile, Fig. 5 delineates the performance of

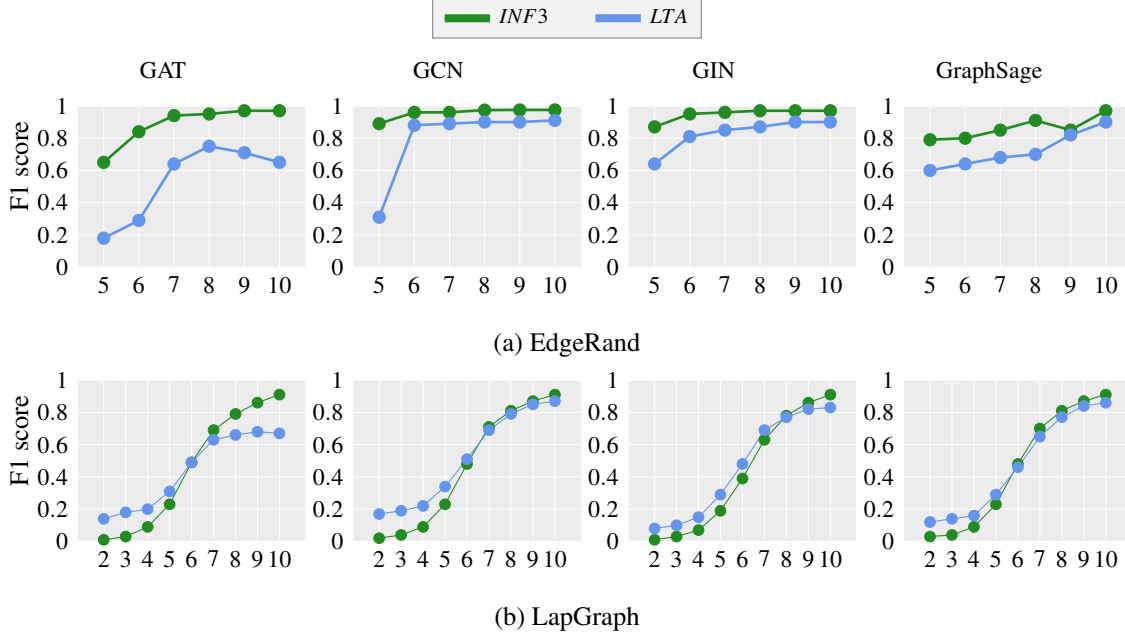


Figure 4: Evaluating *INF3* attack performance on LastFmAsia dataset using EdgeRand and LapGraph privacy defenses. The privacy budgets are presented along the x-axis whereas the attack F1-scores are depicted on the y-axis.

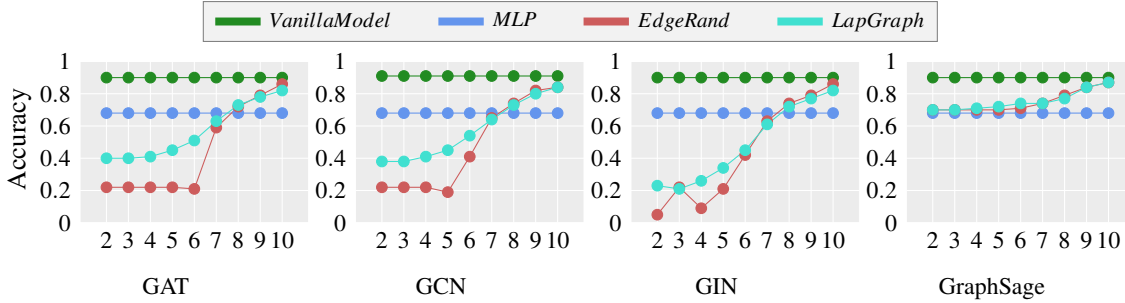


Figure 5: Model performance on LastFmAsia dataset: The x-axis illustrates privacy budgets, and the y-axis shows accuracy.

EdgeRand and LapGraph GNN models alongside MLP and vanilla GNN models. In this study, we regard the MLP model, which is trained solely on node attributes without incorporating edge information, as an ideal defense mechanism. We identify two key observations from the results:

**Observation 1:** The empirical results underscore the challenge of striking a balance between model utility and privacy protection. At a low privacy budget ( $\epsilon < 6$ ), both attacks exhibit poor performance (F1-score  $< 0.6$ ). However, intriguingly, as illustrated in Fig. 5, for GAT, GCN and GIN, both the EdgeRand and LapGraph GNN models lag in usability at lower  $\epsilon$  values, only eclipsing the MLP in performance when  $\epsilon$  escalates to 8 or higher. However, at such high  $\epsilon$  values, the efficacy of the attacks increases and the defense becomes weak (see Fig. 5). While performance degradation is not as pronounced in GraphSAGE consistently outperforming MLP, it still sacrifices a lot of accuracy, compared with vanilla

model, to fortify model privacy (see Fig. 5). This phenomenon underscores the intrinsic trade-off between privacy and utility.

**Observation 2:** *INF3* demonstrates superiority over *LTA* against EdgeRand and achieves better performance than *LTA* against LapGraph when pitted against the defense at high  $\epsilon$  ( $\epsilon \geq 8$ ) (see Fig. 4). It’s important to highlight that for GAT, GCN, and GIN, it is only at  $\epsilon \geq 8$  that the model’s performance surpasses our ideal defense baseline, MLP, as depicted in Fig. 5). The results indicate that, upon reaching a threshold of usable performance, *INF3* consistently eclipses the effectiveness of *LTA*. Moreover, note that, *LTA* and *INF3* have a different threat model. In *LTA*, the adversary directly interacts with the target node pairs, whereas *INF3* allows access only to nodes adjacent to the target, necessitating analysis across a more extended node distance. As messages transfer between nodes with greater distances, more noises get aggregated which can potentially undermine *INF3*’s efficacy.



However, the results show that the amount of noise needed to achieve this also compromises the utility of the GNN model. This highlights the need for an effective defense to mitigate edge privacy leakage.

## 6 Related Work

Attacks on GNN can be classified broadly into two categories: adversarial attacks and privacy attacks. Adversarial attacks [2, 7, 24, 32, 45, 56] aim to reduce the accuracy of the GNN on the classification task and the attack mechanism usually involves poisoning a fraction of the training data of the GNN. In contrast, privacy attacks seek to disclose confidential information about the graph that should only be accessible to the service provider. Based on the information the attacker attempts to extract, the privacy attack against graph data can be categorized into two levels: graph level attack, node/edge level attack, and model level attack [25, 53, 57]. Graph level attack aim ranges from inferring basic properties about the target graph to reconstructing the entire graph [9, 39]. Node/edge level attack [13, 14, 42], on the other hand, focuses on inferring sensitive information about individual nodes or edges. For instance, an attacker may try to infer the gender or age of a particular user in a social network or the existence of friendship between two users. Finally, the trained GNN model is susceptible to model level attacks such as model stealing [8, 31, 41]. In this article, our attention is centered on edge inference attacks; consequently, our literature review is limited to works that are directly related to this topic.

**Edge Inference Attacks on Graphs.** He et al. [13] introduced an attack to infer edges in the training graph in the nodes based on transductive GNNs. This method assumes that connected nodes have similar features and congruent posterior. However, this might not always be the case, potentially compromising the attack’s reliability and consistency. In a separate work, Wu et al. [42] introduce LinkTeller, an attack targeting inductive GNNs. LinkTeller is formulated on the basis of influence analysis. The underlying intuition posits that modifications to a node’s features can disturb the posterior of its adjacent nodes. However, it’s crucial to note that the effectiveness of LinkTeller is bounded by the target GNN’s architecture, exhibiting commendable performance, particularly against Graph Convolutional Networks (GCN) while underperforming against Graph Attention Networks (GAT). Another important factor to note is that LinkTeller employs a distinct threat model compared to our attack. They consider a vertically partitioned graph setting where node features and graph structures originate from separate entities, with the owner of node features acting as the adversary. Contrary to this, GNNBleed does not require the adversary to have knowledge of any node features except the auxiliary nodes they introduced. Moreover, GNNBleed demonstrates superior performance over LinkTeller across all architectures as demonstrated in section 4.3.

**Privacy Preservation in GNN Models.** Various strategies have been introduced to protect the privacy of GNN models, among which Differential Privacy (DP) is notably prevalent. Originating from the foundational work of Dwork *et al.* [10], DP provides a systematic method to uphold privacy, particularly pertinent to machine learning models. It asserts that the outputs of a model when trained on adjacent datasets (those diverging by a single data point at most), should be nearly identical. Typically, DP is achieved by adding appropriately calibrated noise to the result of a function computed on the data. When extending DP to a graph context, notably to edge-level privacy, it has been proposed in varied forms. Two principal methods to embed DP within GNN are identified: Firstly, incorporating DP noise into the graph throughout training and inference phases [42], and secondly, introducing DP noise to each layer during the training process [30]. In this project, we opt to incorporate the approach from [42] due to its facile integration into various models, in contrast to [30], which proposes a specific GNN architecture that doesn’t conveniently meld with widely-used GNN architectures.

**Other Related Privacy Attacks on Graphs.** Duddu *et al.* [9] show that with access to node embeddings trained to preserve graph structure, and a subgraph sampled from the same distribution as the target graph, an attacker can reconstruct the training graph by training an attack model to predict edges based on node embeddings. However, the outlined attack necessitates the attacker to possess extensive information about the GNN, an assumption not deemed realistic. He et al. [14] explored the membership inference attack, which determines if a specific node in the graph was utilized to train the target model by using various foundational knowledge. Nonetheless, this attack method proves to be inefficient in the inductive context, as the target model underwent training on an entirely different graph with no overlapping nodes.

## 7 Conclusion and Future Work

In this paper, we introduce a novel threat model alongside a series of attacks designed for edge inference. We demonstrate that an adversary, having black-box access to a GNN model, can infer the neighbors of a node without requiring direct access to the target nodes’ model predictions. Our design, grounded in the message-passing mechanism in GNN models, is validated through comprehensive evaluations across seven real-world datasets and four distinct GNN architectures, underscoring our attacks’ prowess in achieving notable accuracy and generalization. Future work includes exploring the generalization of our attacks to GNNs deployed for tasks beyond node classification, navigating more complex scenarios such as dynamic graphs where nodes and edges evolve.

## References

- [1] BILOT, T., EL MADHOUN, N., AL AGHA, K., AND ZOUAOUI, A. Graph neural networks for intrusion detection: A survey. *IEEE Access* (2023).
- [2] BOJCHEVSKI, A., AND GÜNNEMANN, S. Adversarial attacks on node embeddings via graph poisoning. In *International Conference on Machine Learning* (2019), PMLR, pp. 695–704.
- [3] CHEN, Y., YANG, H., ZHANG, Y., MA, K., LIU, T., HAN, B., AND CHENG, J. Understanding and improving graph injection attack by promoting unnoticeability, 2022.
- [4] CHU, Y., YAO, J., ZHOU, C., AND YANG, H. Graph neural network in modern recommender systems. In *Graph Neural Networks: Foundations, Frontiers, and Applications*, L. Wu, P. Cui, J. Pei, and L. Zhao, Eds. Springer Singapore, Singapore, 2022, pp. 423–445.
- [5] CORSO, G., CAVALLERI, L., BEAINI, D., LIÒ, P., AND VELIČKOVIĆ, P. Principal neighbourhood aggregation for graph nets. *Advances in Neural Information Processing Systems 33* (2020), 13260–13271.
- [6] DAI, E., ZHAO, T., ZHU, H., XU, J., GUO, Z., LIU, H., TANG, J., AND WANG, S. A comprehensive survey on trustworthy graph neural networks: Privacy, robustness, fairness, and explainability, 2023.
- [7] DAI, H., LI, H., TIAN, T., HUANG, X., WANG, L., ZHU, J., AND SONG, L. Adversarial attack on graph structured data. In *International conference on machine learning* (2018), PMLR, pp. 1115–1124.
- [8] DEFAZIO, D., AND RAMESH, A. Adversarial model extraction on graph neural networks. *arXiv preprint arXiv:1912.07721* (2019).
- [9] DUDDU, V., BOUTET, A., AND SHEJWALKAR, V. Quantifying privacy leakage in graph embedding. In *MobiQuitous 2020 - 17th EAI International Conference on Mobile and Ubiquitous Systems: Computing, Networking and Services* (dec 2020), ACM.
- [10] DWORK, C. Differential privacy. In *International colloquium on automata, languages, and programming* (2006), Springer, pp. 1–12.
- [11] FAN, W., MA, Y., LI, Q., HE, Y., ZHAO, E., TANG, J., AND YIN, D. Graph neural networks for social recommendation. In *The world wide web conference* (2019), pp. 417–426.
- [12] HAMILTON, W. L., YING, R., AND LESKOVEC, J. Inductive representation learning on large graphs, 2018.
- [13] HE, X., JIA, J., BACKES, M., GONG, N. Z., AND ZHANG, Y. Stealing links from graph neural networks, 2020.
- [14] HE, X., WEN, R., WU, Y., BACKES, M., SHEN, Y., AND ZHANG, Y. Node-level membership inference attacks against graph neural networks, 2021.
- [15] JAIN, A., LIU, I., SARDA, A., AND MOLINO, P. Food discovery with uber eats: Using graph learning to power recommendations. Uber, 2019. <https://www.uber.com/en-GR/blog/uber-eats-graph-learning/?ref=assemblyai.com>.
- [16] JEGOROVA, M., KAUL, C., MAYOR, C., O’NEIL, A. Q., WEIR, A., MURRAY-SMITH, R., AND TSAFTARIS, S. A. Survey: Leakage and privacy at inference time, 2022.
- [17] JUMPER, J., EVANS, R., PRITZEL, A., GREEN, T., FIGURNOV, M., RONNEBERGER, O., TUNYASUVUNAKOOL, K., BATES, R., ŽIDEK, A., POTAPENKO, A., ET AL. Highly accurate protein structure prediction with alphafold. *Nature* 596, 7873 (2021), 583–589.
- [18] KIPF, T. N., AND WELLING, M. Semi-supervised classification with graph convolutional networks, 2017.
- [19] KOLLURI, A., BALUTA, T., HOOL, B., AND SAXENA, P. Lpgnet: Link private graph networks for node classification, 2022.
- [20] LEE, J., LEE, I., AND KANG, J. Self-attention graph pooling, 2019.
- [21] LI, G., MÜLLER, M., GHANEM, B., AND KOLTUN, V. Training graph neural networks with 1000 layers. In *International Conference on Machine Learning (ICML)* (2021).
- [22] LI, G., XIONG, C., THABET, A., AND GHANEM, B. Deepergcn: All you need to train deeper gcns, 2020.
- [23] LIU, Y., AO, X., QIN, Z., CHI, J., FENG, J., YANG, H., AND HE, Q. Pick and choose: a gnn-based imbalanced learning approach for fraud detection. In *Proceedings of the web conference 2021* (2021), pp. 3168–3177.
- [24] MA, J., DING, S., AND MEI, Q. Towards more practical adversarial attacks on graph neural networks. *Advances in neural information processing systems 33* (2020), 4756–4766.
- [25] NARAYANAN, A., AND SHMATIKOV, V. De-anonymizing social networks. In *2009 30th IEEE Symposium on Security and Privacy* (may 2009), IEEE.
- [26] RAO, S. X., ZHANG, S., HAN, Z., ZHANG, Z., MIN, W., CHEN, Z., SHAN, Y., ZHAO, Y., AND ZHANG, C. xFraud. *Proceedings of the VLDB Endowment* 15, 3 (nov 2021), 427–436.
- [27] RONG, Y., HUANG, W., XU, T., AND HUANG, J. Dropedge: Towards deep graph convolutional networks on node classification. *arXiv preprint arXiv:1907.10903* (2019).
- [28] ROZEMBERCZKI, B., ALLEN, C., AND SARKAR, R. Multi-scale attributed node embedding, 2021.
- [29] ROZEMBERCZKI, B., AND SARKAR, R. Characteristic functions on graphs: Birds of a feather, from statistical descriptors to parametric models, 2020.
- [30] SAJADMANESH, S., SHAMSABADI, A. S., BELLET, A., AND GATICA-PEREZ, D. Gap: Differentially private graph neural networks with aggregation perturbation. In *32nd USENIX Security Symposium (USENIX Security 23)* (Anaheim, CA, Aug. 2023), USENIX Association.
- [31] SHEN, Y., HE, X., HAN, Y., AND ZHANG, Y. Model stealing attacks against inductive graph neural networks. In *2022 IEEE Symposium on Security and Privacy (SP)* (2022), IEEE, pp. 1175–1192.
- [32] SUN, M., TANG, J., LI, H., LI, B., XIAO, C., CHEN, Y., AND SONG, D. Data poisoning attack against unsupervised node embedding methods. *arXiv preprint arXiv:1810.12881* (2018).
- [33] SUN, Y., WANG, S., TANG, X., HSIEH, T.-Y., AND HONAVAR, V. Adversarial attacks on graph neural networks via node injections: A hierarchical reinforcement learning approach. In *Proceedings of the Web Conference 2020* (2020), pp. 673–683.
- [34] TANG, J., LI, J., GAO, Z., AND LI, J. Rethinking graph neural networks for anomaly detection. In *International Conference on Machine Learning* (2022), PMLR, pp. 21076–21089.
- [35] VAN DEN BERG, R., KIPF, T. N., AND WELLING, M. Graph convolutional matrix completion, 2017.
- [36] VELIČKOVIĆ, P., CUCURULL, G., CASANOVA, A., ROMERO, A., LIÒ, P., AND BENGIO, Y. Graph attention networks, 2018.
- [37] WANG, S., WANG, Z., ZHOU, T., SUN, H., YIN, X., HAN, D., ZHANG, H., SHI, X., AND YANG, J. Threatrace: Detecting and tracing host-based threats in node level through provenance graph learning. *IEEE Transactions on Information Forensics and Security* 17 (2022), 3972–3987.
- [38] WANG, X., CHENG, M., EATON, J., HSIEH, C.-J., AND WU, F. Attack graph convolutional networks by adding fake nodes, 2020.
- [39] WANG, X., AND WANG, W. H. Group property inference attacks against graph neural networks. In *Proceedings of the 2022 ACM SIGSAC Conference on Computer and Communications Security* (New York, NY, USA, 2022), CCS ’22, Association for Computing Machinery, p. 2871–2884.
- [40] WEI, Y., WANG, X., NIE, L., HE, X., HONG, R., AND CHUA, T.-S. Mmgcn: Multi-modal graph convolution network for personalized recommendation of micro-video. In *Proceedings of the 27th ACM international conference on multimedia* (2019), pp. 1437–1445.

- [41] WU, B., YANG, X., PAN, S., AND YUAN, X. Model extraction attacks on graph neural networks: Taxonomy and realisation. In *Proceedings of the 2022 ACM on Asia Conference on Computer and Communications Security* (2022), pp. 337–350.
- [42] WU, F., LONG, Y., ZHANG, C., AND LI, B. Linkteller: Recovering private edges from graph neural networks via influence analysis, 2021.
- [43] WU, S., SUN, F., ZHANG, W., XIE, X., AND CUI, B. Graph neural networks in recommender systems: a survey. *ACM Computing Surveys* 55, 5 (2022), 1–37.
- [44] WU, Z., PAN, S., CHEN, F., LONG, G., ZHANG, C., AND PHILIP, S. Y. A comprehensive survey on graph neural networks. *IEEE transactions on neural networks and learning systems* 32, 1 (2020), 4–24.
- [45] XI, Z., PANG, R., JI, S., AND WANG, T. Graph backdoor. In *30th USENIX Security Symposium (USENIX Security 21)* (2021), pp. 1523–1540.
- [46] XIE, Y., XU, Z., ZHANG, J., WANG, Z., AND JI, S. Self-supervised learning of graph neural networks: A unified review. *IEEE transactions on pattern analysis and machine intelligence* 45, 2 (2022), 2412–2429.
- [47] XU, K., HU, W., LESKOVEC, J., AND JEGELKA, S. How powerful are graph neural networks?, 2019.
- [48] XU, K., LI, C., TIAN, Y., SONOBE, T., KAWARABAYASHI, K.-I., AND JEGELKA, S. Representation learning on graphs with jumping knowledge networks. In *International conference on machine learning* (2018), PMLR, pp. 5453–5462.
- [49] YING, R., HE, R., CHEN, K., EKSOMBATCHAI, P., HAMILTON, W. L., AND LESKOVEC, J. Graph convolutional neural networks for web-scale recommender systems. In *Proceedings of the 24th ACM SIGKDD International Conference on Knowledge Discovery and Data Mining* (jul 2018), ACM.
- [50] YING, R., YOU, J., MORRIS, C., REN, X., HAMILTON, W. L., AND LESKOVEC, J. Hierarchical graph representation learning with differentiable pooling, 2019.
- [51] ZENG, H., ZHANG, M., XIA, Y., SRIVASTAVA, A., MALEVICH, A., KANNAN, R., PRASANNA, V., JIN, L., AND CHEN, R. Decoupling the depth and scope of graph neural networks, 2022.
- [52] ZENG, H., ZHOU, H., SRIVASTAVA, A., KANNAN, R., AND PRASANNA, V. Graphsaint: Graph sampling based inductive learning method, 2020.
- [53] ZHANG, L., AND ZHANG, W. Edge anonymity in social network graphs. In *2009 International Conference on Computational Science and Engineering* (2009), vol. 4, IEEE, pp. 1–8.
- [54] ZHANG, M., AND CHEN, Y. Link prediction based on graph neural networks. *Advances in neural information processing systems* 31 (2018).
- [55] ZHANG, Z., CUI, P., AND ZHU, W. Deep learning on graphs: A survey. *IEEE Transactions on Knowledge and Data Engineering* 34, 1 (2020), 249–270.
- [56] ZHANG, Z., JIA, J., WANG, B., AND GONG, N. Z. Backdoor attacks to graph neural networks. In *Proceedings of the 26th ACM Symposium on Access Control Models and Technologies* (2021), pp. 15–26.
- [57] ZHELEVA, E., AND GETOOR, L. Preserving the privacy of sensitive relationships in graph data. In *Privacy, Security, and Trust in KDD* (Berlin, Heidelberg, 2008), F. Bonchi, E. Ferrari, B. Malin, and Y. Saygin, Eds., Springer Berlin Heidelberg, pp. 153–171.
- [58] ZHOU, J., CUI, G., HU, S., ZHANG, Z., YANG, C., LIU, Z., WANG, L., LI, C., AND SUN, M. Graph neural networks: A review of methods and applications. *AI open* 1 (2020), 57–81.
- [59] ZOU, X., ZHENG, Q., DONG, Y., GUAN, X., KHARLAMOV, E., LU, J., AND TANG, J. TDGIA: Effective injection attacks on graph neural networks. In *Proceedings of the 27th ACM SIGKDD Conference on Knowledge Discovery and Data Mining* (aug 2021), ACM.

Dataset	Nodes	Edges	Features	Classes
Twitch-DE	9,498	315,774	128	2
Twitch-EN	7,126	77,774	128	2
Twitch-ES	4,648	123,412	128	2
Twitch-FR	6,551	231,883	128	2
Twitch-PT	1,912	64,510	128	2
Twitch-RU	4,385	78,993	128	2
Flickr	89,250	899,756	500	7
LastFMAsia	7,624	55,612	128	18

Table 6: Dataset statistics

- [60] ZÜGNER, D., AKBARNEJAD, A., AND GÜNNEMANN, S. Adversarial attacks on neural networks for graph data. In *Proceedings of the 24th ACM SIGKDD International Conference on Knowledge Discovery and Data Mining* (jul 2018), ACM.

## A Additional Information for Evaluation

### A.1 Metrics

Short description of the metrics we used:

**Precision** Precision quantifies how many of the predicted positive instances are genuinely positive. High precision implies that the model returned substantially more true positives than false positives.

**Recall** Recall, on the other hand, quantifies the number of positive instances that the model correctly identified out of all actual positive instances, gauging the model’s completeness. A high recall means the model correctly identified most of the positive instances, with fewer false negatives.

**F1-score** The F1 score strikes a balance between precision and recall, providing a single metric that encapsulates model performance, particularly when there’s an uneven class distribution. Within our attack framework, where connected node pairs are in the minority, the importance of the F1 score becomes paramount.

**ROC-AUC** ROC-AUC, also denoted as simply AUC evaluates the classifier’s ability to differentiate between the classes. A model with a higher AUC can distinguish between the positive and negative classes more effectively.

### A.2 Dataset Statistics

We provide the dataset statistics in Table 6

### A.3 Distance Metrics

The distance metrics utilized for all attacks are enumerated in Table 7.

Table 7: Formulas for various distance metrics.

Metric	Formula
Cosine	$1 - \frac{\mathbf{A} \cdot \mathbf{B}}{\ \mathbf{A}\  \ \mathbf{B}\ }$
Euclidean	$\sqrt{\sum_{i=1}^n (A_i - B_i)^2}$
Correlation	$1 - \frac{\sum (A_i - \bar{A})(B_i - \bar{B})}{\sqrt{\sum (A_i - \bar{A})^2 \sum (B_i - \bar{B})^2}}$
Chebyshev	$\max_i  A_i - B_i $
Bray-Curtis	$\frac{\sum_{i=1}^n  A_i - B_i }{\sum_{i=1}^n (A_i + B_i)}$
Canberra	$\sum_{i=1}^n \frac{ A_i - B_i }{ A_i + B_i }$
Manhattan	$\sum_{i=1}^n  A_i - B_i $
Square-Euclidean	$\sum_{i=1}^n (A_i - B_i)^2$

## B Additional Experiment Results

### B.1 Full Result for SIM and INF2 Using Different Distance Metrics

The full result for SIM and INF2 with different distance metrics are available in Table B.1.

Table 8: F1 Score of SIM and INF2 Attack with Different Distance Metrics

Dataset	Metric	SIM				INF2			
		GCN	SAGE	GAT	GIN	GCN	SAGE	GAT	GIN
LastFmAsia	Cosine	0.55	0.39	0.45	0.37	0.73	0.67	0.67	0.97
	Euclidean	0.44	0.33	0.39	0.34	0.64	0.60	0.59	0.97
	Correlation	0.55	0.40	0.47	0.37	0.96	0.83	0.74	0.97
	Chebyshev	0.51	0.35	0.43	0.35	0.62	0.60	0.61	0.97
	Bray-Curtis	0.42	0.30	0.36	0.31	0.93	0.89	0.84	0.97
	Canberra	0.44	0.30	0.35	0.31	0.96	0.95	0.89	0.97
	Manhattan	0.42	0.30	0.38	0.33	0.64	0.60	0.59	0.97
	Square-Euclidean	0.44	0.30	0.39	0.34	0.64	0.60	0.59	0.97
	Flickr	Cosine	0.31	0.19	0.34	0.24	0.83	0.76	0.84
Euclidean		0.29	0.18	0.35	0.23	0.70	0.70	0.67	1.0
Correlation		0.32	0.19	0.33	0.23	0.84	0.76	0.83	1.0
Chebyshev		0.29	0.18	0.35	0.24	0.70	0.69	0.67	1.0
Bray-Curtis		0.28	0.20	0.34	0.22	0.99	0.83	0.99	1.0
Canberra		0.28	0.18	0.37	0.23	0.99	0.95	0.99	1.0
Manhattan		0.28	0.18	0.34	0.22	0.70	0.70	0.67	1.0
Square-Euclidean		0.29	0.18	0.35	0.23	0.70	0.70	0.67	1.0

### B.2 Target Node degree distribution

In our study, we categorize target nodes across various datasets based on their degree of connectivity:

*Unconstrained Subset:* We include nodes from the complete testing graph, provided they have more than three connections.

*Specific Degree Subsets:* For Twitch & LastFm, nodes with a degree of 5 or less are considered low degree, whereas those with a degree of 10 or more are deemed high degree. For Flickr, because it is a larger graph, we adjust the thresholds, categorizing nodes with up to 15 connections as low degree and those with 30 or more as high degree.

## B.3 Auxiliary Node Feature Selection

The full result for different auxiliary node feature can be found in Table 9.

## B.4 Experiment Result

More result about the performance of INF3 attack on target nodes with different degree distributions and threshold estimation is available in Table 10

## C Additional Attacks

**Similarity Attack 2 (SIM2)** This attack explores the relationship between node posterior similarity and node distance from the point of change in architecture. This attack method capitalizes on the theory asserting that the similarity between the posteriors of two nodes, which are proximate within the graph, should maintain relative consistency even when they are artificially brought closer together. The adversary can integrate new edges involving auxiliary nodes and then scrutinize variations in the distances between the posteriors of these nodes. Initially, we introduce two nodes,  $a_1$  and  $a_2$ , with identical features into the graph, forming edges  $(t, a_1)$  and  $(c, a_2)$  respectively. Consequently, we can obtain the posteriors  $p_{a_1}$  and  $p_{a_2}$ . Following this, we form a new edge  $(c, a_1)$ , effectively reducing the distance between  $a_1$  and  $a_2$  to two, and consequently obtain  $p'_{a_1}$  and  $p'_{a_2}$ . We then compute the distances between  $(p_{a_1}, p_{a_2})$  and  $(p'_{a_1}, p'_{a_2})$ , employing the shift in distance as a statistical measure to infer edges. The underlying inference is that the more marginal the alteration in distance, the higher the probability of an existing connection between nodes  $t$  and  $c$ . Additional details of our algorithm can be found in Algorithm 6.

### Algorithm 6 Similarity Attack 2 (SIM2)

**Input:** Node Pair  $(t, c)$ , Distance Metrics  $DistanceMetrics(\cdot, \cdot)$ , Graph  $G$   
**Output:** a score which quantifies the likelihood that  $t$  and  $c$  are connected  
1:  $G' \leftarrow$  adding two auxiliary nodes  $a_1$  and  $a_2$  to  $G$ , and establishing edges  $(t, a_1)$  and  $(c, a_2)$ , respectively.  
2:  $P \leftarrow GNN(G')$   
3:  $G'' \leftarrow$  create an edge  $(c, a_1)$   
4:  $P' \leftarrow M(G'')$   
5: **return**  $DistanceMetrics(P'[a_1], P'[a_2]) - DistanceMetrics(P[a_1], P[a_2])$



Table 9: Performance of the *INF3* Attack with Varied Inserted Node Features: Groupings of rows indicate inserted nodes characterized by different features.

<b>Model</b>	<b>Node Feature</b>	<b>LastFmAsia</b>	<b>Flickr</b>	<b>Twitch-DE</b>	<b>Twitch-RU</b>	<b>Twitch-PT</b>	<b>Twitch-FR</b>	<b>Twitch-EN</b>
GCN	Random	0.976	1.0	0.992	1.0	0.996	0.993	0.996
	Typical	0.976	1.0	0.972	0.908	0.996	0.996	0.996
	Duplication	0.976	1.0	0.987	0.988	0.996	0.986	0.996
	Mean	0.936	1.0	0.965	0.988	0.996	0.996	0.996
	Median	0.976	1.0	0.972	0.988	0.996	0.996	0.996
GAT	Random	0.938	1.0	0.899	0.961	0.996	0.959	0.976
	Typical	0.966	1.0	0.981	0.986	0.996	0.987	0.976
	Duplication	0.969	1.0	0.944	0.953	0.996	0.954	0.976
	Mean	0.963	0.999	0.960	0.988	0.996	0.959	0.940
	Median	0.963	0.999	0.979	0.961	0.996	0.968	0.994
SAGE	Random	0.976	1.0	0.969	0.983	0.945	0.947	0.983
	Typical	0.976	1.0	0.973	0.971	0.929	0.973	0.977
	Duplication	0.976	1.0	0.968	0.973	0.957	0.962	0.983
	Mean	0.751	0.992	0.962	0.973	0.945	0.958	0.964
	Median	0.976	0.999	0.967	0.974	0.963	0.973	0.981
GIN	Random	0.976	1.0	1.0	0.999	0.996	0.996	0.996
	Typical	0.976	1.0	1.0	0.999	0.996	0.996	0.996
	Duplication	0.976	1.0	1.0	0.999	0.996	0.996	0.996
	Mean	0.977	1.0	1.0	0.999	0.996	0.996	0.996
	Median	0.976	1.0	1.0	0.999	0.996	0.996	0.996

Table 10: Performance of INF3 attack on target nodes with different degree distributions and threshold estimation.

(a) Twitch-EN

$\hat{d}$	Model	Low Degree		Unconstrained		High Degree	
		Recall	Precision	Recall	Precision	Recall	Precision
[0.8d]	GCN	0.718	0.994	0.748	0.996	0.782	0.999
	SAGE	0.716	0.991	0.748	0.996	0.780	0.997
	GAT	0.713	0.988	0.741	0.986	0.773	0.988
	GIN	0.686	0.952	0.717	0.966	0.798	0.998
d	GCN	0.995	0.995	0.996	0.996	0.999	0.999
	SAGE	0.966	0.966	0.981	0.981	0.972	0.972
	GAT	0.971	0.971	0.976	0.976	0.973	0.973
	GIN	0.966	0.966	0.996	0.996	0.998	0.998
[1.2d]	GCN	1.0	0.809	1.0	0.821	1.0	0.845
	SAGE	0.997	0.817	0.995	0.849	0.988	0.872
	GAT	0.997	0.808	0.995	0.820	0.995	0.820
	GIN	1.0	0.996	1.0	0.997	1.0	0.999

(b) Twitch-FR

$\hat{d}$	Model	Low Degree		Unconstrained		High Degree	
		Recall	Precision	Recall	Precision	Recall	Precision
[0.8d]	GCN	0.737	0.999	0.767	0.997	0.790	0.997
	SAGE	0.723	0.993	0.749	0.971	0.776	0.982
	GAT	0.734	0.990	0.763	0.990	0.784	0.992
	GIN	0.737	0.995	0.767	0.995	0.790	1.0
d	GCN	0.996	0.996	0.993	0.993	0.996	0.996
	SAGE	0.965	0.965	0.941	0.941	0.955	0.955
	GAT	0.978	0.978	0.959	0.959	0.951	0.951
	GIN	0.996	0.996	0.992	0.992	0.994	0.994
[1.2d]	GCN	1.0	0.820	0.996	0.822	0.996	0.828
	SAGE	0.988	0.824	0.971	0.832	0.965	0.846
	GAT	0.986	0.822	0.971	0.818	0.968	0.825
	GIN	1.0	0.997	0.995	0.997	1.0	0.997

(c) Twitch-PT

$\hat{d}$	Model	Low Degree		Unconstrained		High Degree	
		Recall	Precision	Recall	Precision	Recall	Precision
[0.8d]	GCN	0.730	0.991	0.767	1.0	0.788	1.0
	SAGE	0.719	0.978	0.760	0.993	0.779	0.991
	GAT	0.683	0.930	0.680	0.862	0.663	0.843
	GIN	0.730	0.991	0.767	1.0	0.788	1.0
d	GCN	0.994	0.994	0.999	0.999	1.0	1.0
	SAGE	0.961	0.961	0.943	0.943	0.943	0.943
	GAT	0.841	0.841	0.818	0.818	0.806	0.806
	GIN	0.994	0.994	0.999	0.999	1.0	1.0
[1.2d]	GCN	1.0	0.797	1.0	0.812	1.0	0.825
	SAGE	0.990	0.798	0.953	0.810	0.951	0.818
	GAT	0.917	0.730	0.919	0.747	0.904	0.747
	GIN	1.0	0.997	1.0	1.0	1.0	1.0